Effect of Long-Distance Electron Transfer on Chemiluminescence Efficiencies

Robert D. Mussell and Daniel G. Nocera*

Contribution from the Department of Chemistry, Michigan State University, East Lansing, Michigan 48824. *Received March 23, 1987. Revised Manuscript Received October 23, 1987*

Abstract: The electrogenerated chemiluminescence (ecl) of $Mo_6Cl_{14}^{2-}$ with three series of structurally and electronically related electroactive organic compounds in acetonitrile has been investigated. The yields for the formation of the electronically excited $Mo_6Cl_{14}^{2-}$ ion produced by the electron-transfer reaction of $Mo_6Cl_{14}^{3-}$ with aromatic amine radical cations (A^+) and by the reaction of $Mo_6Cl_{14}^-$ with nitroaromatic radical anions (D^-) and pyridinium radicals (D) have been measured over a wide potential range by simply varying the reduction potential of the electroactive organic reagent. The dependence of the formation yield of $Mo_6Cl_{14}^{2-*}$, ϕ_{es}, on the driving force of the annihilation reaction is similar for the three series. ϕ_{es} is immeasurable ($<10^{-6}$) for reactions with free energies positive of a threshold value. Over a narrow free energy range just negative of threshold, ϕ_{es} rapidly increases. And with increasing exergonicity of the electron-transfer reaction, ϕ_{es} asymptotically approaches a limiting value less than unity [$\phi_{es}^{lim}(Mo_6Cl_{14}^-/D^-) = 0.013 \pm 0.001$; $\phi_{es}^{lim}(Mo_6Cl_{14}^-/D) = 0.079 \pm 0.008$; $\phi_{es}^{lim}(Mo_6Cl_{14}^{3-}/A^+) = 0.132 \pm 0.006$]. Analysis of these excited-state production yields by Marcus theory suggests that unit efficiencies for excited-state production are circumvented by long-distance electron transfer.

The formation of products in luminescent excited states may result from highly exergonic electron-transfer reactions of chemically generated (chemiluminescence, cl) or electrogenerated (electrogenerated chemiluminescence, ecl) intermediates. One of the principal themes that has emerged from mechanistic considerations of ecl and cl reactions is that the efficiency of excited-state production is related intimately to the energetics of electron transfer. Extensive investigations of ecl and cl reactivity have established two schemes for excited-state production:[1-7] the emitting state is formed directly upon electron transfer (S-route) or the emitting state is produced by an upconversion reaction involving an intermediate excited state formed in the electron-transfer reaction (T-route). For typical organic ecl or cl systems, the high energy of the luminescent excited state (usually a singlet) precludes S-route reactivity and electron transfer produces a nonemissive triplet intermediate, which undergoes annihilation to yield the emitting singlet state. Because triplet-triplet annihilation processes are inherently inefficient,[8] the excited-state production yields of organic systems are generally limited to a few percent.[6a,9-11] In contrast, luminescence from transition-metal complexes usually originates from the lowest energy electronic excited state, and therefore S-route reactivity for inorganic species is governed by modest energies. In recent years, ecl and cl from a variety of inorganic compounds including $M(bpy)_3^{2+}$ (M = Ru, Os; bpy = 2,2'-bipyridine)[12,13] and related species,[14-16] Re(I) diimine complexes,[17] binuclear complexes possessing metal-metal bonds,[18,19] phthalocyanines,[20] and square-planar complexes of Pd(II)[21] and Pt(II)[22] have been reported. For all of these systems, the energy released from the electron-transfer reaction between oxidized and reduced forms of the parent molecule (i.e., commonly called the annihilation reaction) is sufficiently energetic to directly populate the luminescent excited state. Nevertheless, despite this predicted and in some cases experimentally verified S-route behavior,[23,24] measured efficiencies for excited-state production are well below unity.[25] The reasons for the low yields of some of these systems are known. For example, an ecl yield of $<10^{-5}$ for the $Pt_2(H_2P_2O_5)_4^{4-}$ system[26] can most certainly be attributed to the relatively short lifetime of $Pt_2(H_2P_2O_5)_5^{5-}$ in aqueous solution.[27] And low excited-state yields of RuL_3^{2+*} (L = polypyridyl) produced in the reaction of RuL_3^{3+} with CoL_3^+ ions have been shown to result from an electron-transfer pathway competitive to cl in which a nonluminescent excited state of CoL_3^{2+} is populated.[28] For the most part, however, a general understanding of the low ecl and cl yields of inorganic systems has not been achieved.

Yields for the production of electronically excited transition-metal complexes are of considerable interest from a practical standpoint[29-33] and also because they can provide insight into

(1) Faulkner, L. R.; Bard, A. J. *J. Am. Chem. Soc.* **1969**, *91*, 209-210.
(2) Bezman, R.; Faulkner, L. R. *J. Am. Chem. Soc.* **1972**, *94*, 6317-6323.
(3) (a) Hercules, D. M. *Acc. Chem. Res.* **1969**, *2*, 301-306. (b) Hercules, D. M. *Physical Methods in Organic Chemistry*; Weissberger, A.; Rossiter, B., Eds.; Academic: New York, 1971; Part II, Chapter 13.
(4) Chandross, E. A. *Trans. N.Y. Acad. Sci.* **1969**, *31*, 571-583.
(5) Weller, A.; Zachariasse, K. *Chemiluminescence and Bioluminescence*; Cormier, M.; Hercules, D. M.; Lee, J., Eds.; Plenum: New York, 1973.
(6) (a) Faulkner, L. R. *Int. Rev. Sci.: Phys. Chem., Ser. Two* **1975**, *9*, 213-263. (b) Faulkner, L. R. *Methods Enzymol.* **1978**, *57*, 494-526. (c) Faulkner, L. R.; Glass, R. S. *Chemical and Biological Generation of Excited States*; Adam, W.; Gilento, G., Eds.; Academic: New York, 1982.
(7) Park, S.-M.; Tryk, D. A. *Rev. Chem. Intermed.* **1981**, *4*, 43-79.
(8) Turro, N. J. *Modern Molecular Photochemistry*; Benjamin/Cummings: Menlo Park, CA, 1978.
(9) Pighin, A. *Can. J. Chem.* **1973**, *51*, 3467-3472.
(10) Bard, A. J.; Keszthelyi, C. P.; Tachikawa, H.; Tokel, N. E. *Chemiluminescence and Bioluminescence*; Cormier, M.; Hercules, D. M., Lee, J., Eds.; Plenum: New York, 1973.
(11) (a) Itoh, K.; Honda, K.; Sukigara, M. *Electrochim. Acta* **1979**, *24*, 1195-1198. (b) Itoh, K.; Honda, K.; Sukigara, M. *J. Electroanal. Chem.* **1980**, *110*, 277-284.
(12) Tokel, N. E.; Bard, A. J. *J. Am. Chem. Soc.* **1972**, *94*, 2862-2863.
(13) Abruna, H. D. *J. Electroanal. Chem.* **1984**, *175*, 321-326.
(14) Tokel-Takvoryan, N. E.; Bard, A. J. *J. Am. Chem. Soc.* **1973**, *95*, 6582-6589.
(15) Abruna, H. D. *J. Electrochem. Soc.* **1985**, *132*, 842-849.
(16) Gonzales-Velasco, J.; Rubinstein, I.; Crutchley, R. J.; Lever, A. B. P.; Bard, A. J. *Inorg. Chem.* **1983**, *22*, 822-825.
(17) Luong, J. C.; Nadjo, L.; Wrighton, M. S. *J. Am. Chem. Soc.* **1978**, *100*, 5790-5795.
(18) Vogler, A.; Kunkely, H. *Angew. Chem., Int. Ed. Engl.* **1984**, *23*, 316-317.
(19) Ouyang, J.; Zietlow, T. C.; Hopkins, M. D.; Fan, F.-R. F.; Gray, H. B.; Bard, A. J. *J. Phys. Chem.* **1986**, *90*, 3841-3844.
(20) Wheeler, B. L.; Nagasubramanian, G.; Bard, A. J.; Schechtman, L. A.; Dininny, D. R.; Kenney, M. E. *J. Am. Chem. Soc.* **1984**, *106*, 7404-7410.
(21) Tokel-Takvoryan, N. E.; Bard, A. J. *Chem. Phys. Lett.* **1974**, *25*, 235-238.
(22) Bonafede, S.; Ciano, M.; Bolletta, F.; Balzani, V.; Chassot, L.; Zelewsky, A. *J. Phys. Chem.* **1986**, *90*, 3836-3841.
(23) Luttmer, J. D.; Bard, A. J. *J. Phys. Chem.* **1981**, *85*, 1155-1159.
(24) Glass, R. S.; Faulkner, L. R. *J. Phys. Chem.* **1981**, *85*, 1160-1165.
(25) (a) With the exception of $Ru(bpy)_3^{2+}$ at low temperatures,[25b,c] the excited-state production yields of all transition-metal complexes exhibiting cl and ecl are less than unity. (b) Wallace, W. L.; Bard, A. J. *J. Phys. Chem.* **1979**, *83*, 1350-1357. (c) Itoh, K.; Honda, K. *Chem. Lett.* **1979**, 99-102.
(26) Kim, J.; Fan, F. F.; Bard, A. J.; Che, C.-M.; Gray, H. B. *Chem. Phys. Lett.* **1985**, *121*, 543-546.
(27) Che, C.-M.; Atherton, S. J.; Butler, L. G.; Gray, H. B. *J. Am. Chem. Soc.* **1984**, *106*, 5143-5145.
(28) Liu, D. K.; Brunschwig, B. S.; Creutz, C.; Sutin, N. *J. Am. Chem. Soc.* **1986**, *108*, 1749-1755.

0002-7863/88/1510-2764$01.50/0

mechanistic features of highly exergonic electron transfer.[34-37] Classical[38,39] and quantum mechanical[40-46] treatments of electron transfer predict that the reaction rate will increase with increasing negative free energy, maximize for moderately exergonic reactions, and thereafter decrease as the standard free energy becomes more negative. While numerous experimental studies have provided ample data which support an increase and leveling of the rate with increasing free energy (i.e., the normal electron-transfer region),[47-53] observation of a decrease in rate at high exergonicities (i.e., the inverted region) has proven experimentally more elusive, especially for bimolecular reactions in homogeneous solution.[54] For a chemiluminescent system, electron transfer between oxidized and reduced reactants in the normal region leads to the population of the emissive excited state whereas reaction to directly yield ground-state products occurs in the inverted region. In this regard, cl is a convenient chemical marker of electron-transfer pathways, and measurements of cl and ecl quantum yields (ϕ_{cl} or ϕ_{ecl} = photons emitted/electrons transferred) provide direct information on the relative rates for bimolecular electron transfer in the normal and inverted regions.

Our interest in cl has centered on the electron-transfer chemistry of the hexanuclear cluster ion $Mo_6Cl_{14}^{2-}$ in nonaqueous solution. Ecl of $Mo_6Cl_{14}^{2-}$ is produced by the electron-transfer reaction between $Mo_6Cl_{14}^{-}$ and $Mo_6Cl_{14}^{3-}$.[55] The magnitudes of the $Mo_6Cl_{14}^{-/2-}$ and $Mo_6Cl_{14}^{2-/3-}$ reduction couples [$E_{1/2}(Mo_6Cl_{14}^{-/2-})$ = +1.53 V vs SCE, $E_{1/2}(Mo_6Cl_{14}^{2-/3-})$ = -1.56 V vs SCE in CH_3CN] and the relatively low energy of the $Mo_6Cl_{14}^{2-}$ excited state [$E_{em}(Mo_6Cl_{14}^{2-*})$ = 1.9 V] have allowed us to observe ecl from the annihilation of $Mo_6Cl_{14}^{-}$ and $Mo_6Cl_{14}^{3-}$ with a variety of electroactive donors (e.g., nitroaromatic radical anions) and acceptors (e.g., aromatic amine radical cations), respectively.[56] When the reduction potential of the electroactive donor or acceptor is varied, the ecl dynamics of $Mo_6Cl_{14}^{2-}$ ion can systematically be investigated over a wide potential energy range. We now report the dependence of ecl quantum yields on the exergonicity of the electron-transfer reactions of $Mo_6Cl_{14}^{-}$ with a series of nitroaromatic radical anions (D^-) and pyridinium radicals (D) and the reaction of $Mo_6Cl_{14}^{3-}$ with aromatic amine cations (A^+). Analysis of these yields in the context of electron-transfer theories suggests that efficient ecl is circumvented by long-distance electron transfer. Our results may explain the low excited-state yields for the chemiluminescent reactions of other inorganic complexes.

Experimental Section

Materials. The tetrabutylammonium salt of $Mo_6Cl_{14}^{2-}$ was prepared and purified by previously described methods.[57] Nitroaromatics and aromatic amines, with the exception of tri-*p*-tolylamine, which was synthesized following published procedures,[58] were obtained from commercial sources (Aldrich Chemical Co., Alfa Products, and Pfaltz and Bauer). Solids were purified by recrystallization followed by vacuum sublimation, and liquids were purified by fractional distillation. The pyridinium salts were synthesized by addition of either methyl iodide or benzyl chloride to a 1:1 acetone/ethanol solution of the appropriately substituted pyridine. Isonicotinamide (Sigma), 4-cyanopyridine (Aldrich), and isonicotinic acid ethyl ester (Sigma) were used without subsequent purification. Pyridinium hexafluorophosphate salts, obtained by the addition of ammonium hexafluorophosphate to aqueous solutions of the chloro or iodo salts, were twice recrystallized from acetone/water solutions. Tetrabutylammonium perchlorate and hexafluorophosphate (Southwestern Analytical Chemicals) were dissolved in ethyl acetate, dried over $MgSO_4$, recrystallized from pentane–ethyl acetate solution, and dried in vacuo for 12 h at 60 °C. Acetonitrile, obtained from Burdick and Jackson Laboratories (distilled in glass grade), was subjected to seven freeze–pump–thaw (fpt) cycles and vacuum distilled onto 3-Å molecular sieves contained in a 1-L flask equipped with a high-vacuum Teflon valve.

Electrochemical Measurements. Formal reduction potentials of acceptors and donors were determined by cyclic voltammetry with a Princeton Applied Research (PAR) Model 173 potentiostat, Model 175 programmer, and a Model 179 digital coulometer. The output of the digital coulometer was fed directly into a Houston Instrument Model 2000 X-Y recorder. A three-electrode system was used with a standard H-cell configuration. The working electrode was a Pt button, the auxiliary electrode was a Pt gauze, and a Ag wire served as an adequate reference potential by using ferrocene as an internal standard.[59] Potentials were related to the SCE reference scale by using a ferrocenium–ferrocene couple of 0.31 V vs SCE.

Quenching Experiments. Quenching rate constants for reaction of $Mo_6Cl_{14}^{2-*}$ with donors and acceptors in CH_3CN ($[(Bu_4N)_2Mo_6Cl_{14}]$ = 3 mM, μ = 0.1 M NBu_4ClO_4) were determined from Stern–Volmer plots of the $Mo_6Cl_{14}^{2-}$ luminescence intensity. Stern–Volmer experiments were performed over a quencher concentration range of 10^{-3}–10^{-1} M, and Stern–Volmer constants were calculated with $\tau_0(Mo_6Cl_{14}^{2-*})$ = 180 μs in CH_3CN at 25 °C. A specially constructed high-vacuum cell, consisting of a 1-cm quartz cuvette attached to a side arm terminating with a 10-mL round-bottomed flask, permitted all quencher additions to be performed under high-vacuum conditions.

Luminescence intensities were measured on an emission spectrometer constructed at Michigan State University. The excitation beam of the emission spectrometer originates from a 200-W Hg–Xe lamp, mounted

(29) (a) Schaper, H.; Schnedler, E. *J. Phys. Chem.* **1982**, *86*, 4380–4385. (b) Schaper, H.; Koestlin, H.; Schnedler, E. *Philips Tech. Rev.* **1982**, *40*, 69–80.

(30) (a) Laser, D.; Bard, A. J. *J. Electrochem. Soc.* **1975**, *122*, 632–640. (b) Brilmyer, G. H.; Bard, A. J. *J. Electrochem. Soc.* **1980**, *127*, 104–110.

(31) Heller, C. A.; Jernigan, J. L. *Appl. Opt.* **1977**, *16*, 61–66.

(32) Measures, R. M. *Appl. Opt.* **1974**, *13*, 1121–1133; **1975**, *14*, 909–916.

(33) Schuster, G. B. *J. Am. Chem. Soc.* **1979**, *101*, 5851–5853.

(34) Siders, P.; Marcus, R. A. *J. Am. Chem. Soc.* **1981**, *103*, 748–752.

(35) Bock, C. R.; Connor, J. A.; Gutierrez, A. R.; Meyer, T. J.; Whitten, D. G.; Sullivan, B. P.; Nagle, J. K. *J. Am. Chem. Soc.* **1979**, *101*, 4815–4824.

(36) Meyer, T. J. *Prog. Inorg. Chem.* **1983**, *30*, 389–440.

(37) Bolletta, F.; Bonafede, S. *Pure Appl. Chem.* **1986**, *58*, 1229–1232.

(38) Marcus, R. A. *Discuss. Faraday Soc.* **1960**, *29*, 21–31.

(39) For reviews, see: (a) Sutin, N. *Prog. Inorg. Chem.* **1983**, *30*, 441–498. (b) Newton, M. D.; Sutin, N. *Annu. Rev. Phys. Chem.* **1984**, *35*, 437–480.

(40) (a) Van Duyne, R. P.; Fischer, S. F. *Chem.* Phys. **1974**, *5*, 183–197. (b) Fischer, S. F.; Van Duyne, R. P. *Chem. Phys.* **1977**, *26*, 9–16.

(41) Kestner, N. R.; Logan, J.; Jortner, J. *J. Phys. Chem.* **1974**, *78*, 2148–2165.

(42) (a) Ulstrup, J.; Jortner, J. *J. Chem. Phys.* **1975**, *63*, 4358–4368. (b) Jortner, J.; Ulstrup, J. *J. Am. Chem. Soc.* **1979**, *101*, 3744–3754.

(43) Brunschwig, B. S.; Logan, J.; Newton, M. D.; Sutin, N. *J. Am. Chem. Soc.* **1980**, *102*, 5798–5809.

(44) Newton, M. D. *Int. J. Quantum Chem.* **1980**, *14*, 364–391.

(45) Webman, I.; Kestner, N. R. *J. Chem. Phys.* **1982**, *77*, 2387–2398.

(46) (a) Siders, P.; Marcus, R. A. *J. Am. Chem. Soc.* **1981**, *103*, 741–747. (b) Siders, P.; Cave, R. J.; Marcus, R. A. *J. Chem. Phys.* **1984**, *81*, 5613–5624.

(47) Rehm, D.; Weller, A. *Isr. J. Chem.* **1970**, *8*, 259–271.

(48) (a) Creutz, C.; Sutin, N. *J. Am. Chem. Soc.* **1977**, *99*, 241–243. (b) Lin, C.-T.; Bottcher, W.; Chou, M.; Creutz, C.; Sutin, N. *J. Am. Chem. Soc.* **1976**, *98*, 6536–6544.

(49) (a) Ballardini, R.; Varani, G.; Indelli, M. T.; Scandola, F.; Balzani, V. *J. Am. Chem. Soc.* **1978**, *100*, 7219–7223. (b) Scandola, F.; Balzani, V.; Schuster, G. B. *J. Am. Chem. Soc.* **1981**, *103*, 2519–2523. (c) Indelli, M. T.; Ballardini, R.; Scandola, F. *J. Phys. Chem.* **1984**, *88*, 2547–2551.

(50) Nagle, J. K.; Dressick, W. J.; Meyer, T. J. *J. Am. Chem. Soc.* **1979**, *101*, 3993–3995.

(51) (a) Nocera, D. G.; Gray, H. B. *J. Am. Chem. Soc.* **1981**, *103*, 7349–7350. (b) Marshall, J. L.; Stobart, S. R.; Gray, H. B. *J. Am. Chem. Soc.* **1984**, *106*, 3027–3029.

(52) Heuer, W. B.; Totten, M. D.; Rodman, G. S.; Hebert, E. J.; Tracy, H. J.; Nagle, J. K. *J. Am. Chem. Soc.* **1984**, *106*, 1163–1164.

(53) Kavarnos, G. J.; Turro, N. J. *Chem. Rev.* **1986**, *86*, 401–449.

(54) Unequivocal evidence of the inverted region for intramolecular electron-transfer reactions has recently been presented.[54b-e] (b) Miller, J. R.; Calcaterra, L. T.; Closs, G. L. *J. Am. Chem. Soc.* **1984**, *106*, 3047–3049. (c) Miller, J. R.; Beitz, J. V.; Huddleston, R. K. *J. Am. Chem. Soc.* **1984**, *106*, 5057–5068. (d) Closs, G. L.; Calcaterra, L. T.; Green, N. J.; Penfield, K. W.; Miller, J. R. *J. Phys. Chem.* **1986**, *90*, 3673–3683. (e) Wasielewski, M. P.; Niemczyk, M. P.; Svec, W. A.; Pewitt, E. B. *J. Am. Chem. Soc.* **1985**, *107*, 1080–1082.

(55) Nocera, D. G.; Gray, H. B. *J. Am. Chem. Soc.* **1984**, *106*, 824–825.

(56) Mussell, R. D.; Nocera, D. G. *Polyhedron* **1986**, *5*, 47–50.

(57) Sheldon, J. C. *J. Chem. Soc.* **1960**, 1007–1014.

(58) Walter, R. I. *J. Am. Chem. Soc.* **1955**, *77*, 5999–6002.

(59) Gagne, R. R.; Koval, C. A.; Lisensky, G. C. *Inorg. Chem.* **1980**, *19*, 2854–2855.

in a Spex 1909 lamp housing ($f/4$), and is focused onto the entrance slit of a Spex 1680A double monochromator (0.22 m, $f/4$). The wavelength-selected excitation light, collimated by a $f/4$ fused silica lens, passes through an Oriel 436-nm interference filter (Oriel) and is focused onto the sample cell with a $f/1$ fused silica lens. Light emitted from the sample is collected at 90° to the excitation beam with a collimating lens ($f/1.5$) and then is focused by a second lens ($f/8$) through a Corion color glass cutoff filter onto the entrance slit of a Spex 0.5-m 1870B monochromator ($f/8$). The wavelength scan of the monochromator is controlled by a Spex 1673C Mini-Drive 2. The dispersed emission is detected by a Hamamatsu R1104 photomultiplier tube, which is cooled to −70 °C in a Products for Research Model TE241RF housing. The spectral responses of the monochromator and PMT were calibrated with a standard of spectral irradiance 45-W tungsten halogen lamp from Optronics Laboratories. The lamp spectrum was recorded at a constant current of 6.500 ± 0.0002 A, and corrections in 0.1-Å intervals from 250 to 1500 nm were made with the spectral irradiance profile of the lamp provided by Optronics. The signal from the photomultiplier tube is passed through a LeCroy VV100B single-channel fast-pulse amplifier to the input of an EG&G Model 128A lock-in amplifier. The input signal to the lock-in amplifier is phase matched to the reference signal generated by a PAR Model 125A light chopper situated between the excitation monochromator and the sample chamber. The output from the lock-in amplifier may be fed directly into a Soltec Model 124A strip chart recorder and/or collected in digital format by a Zenith ZQ-151-52 microcomputer. The computer interface utilizes a gated output from the Spex Mini-Drive 2 to initiate a Metrabyte Corp. DSH-16 Data Acquisition Board, which is responsible for A/D conversion in 0.1-Å increments.

Electrogenerated Chemiluminescence. A triple-step square-wave potential sequence generated by the PAR 175 programmer was used to establish ecl reactions. The potential limits of the program sequence were chosen to ensure production of electrogenerated intermediates in the mass-transfer-controlled region. The electrochemical cell employed in ecl measurements was a cylindrical, single-compartment high-vacuum cell. A side arm permitted solvents to be transferred into the cell by vacuum distillation, and two sample chargers allowed cluster and electroactive acceptor or donor to be added independently to the working electrode compartment while the isolated environment of the electrochemical cell is maintained. Two tungsten wires sealed in uranium glass served as electrical leads for a Pt mesh auxiliary electrode and a Ag wire quasi-reference electrode. The auxiliary and reference electrodes were positioned parallel to a Pt disk working electrode (A = 0.0314 cm^2), which was positioned centrosymmetrically along the cylindrical axis of the working compartment. The Pt disk was spectroscopically viewed through a fused silica window, which constituted the bottom surface of the electrochemical cell.

Ecl spectra and quantum yield experiments were performed in CH_3CN solution containing 0.1 M supporting electrolyte and equimolar concentrations of $Mo_6Cl_{14}^{2-}$ and electroactive acceptor or donor. Samples for all ecl experiments were prepared by transferring 3.5 mL of solvent under a high-vacuum manifold (5×10^{-7}–1×10^{-6} Torr) into the cell side arm which contained supporting electrolyte predried at 100 °C for 4 h. After three fpt cycles, the solution was thoroughly mixed and poured into the working chamber by slowly rotating the cell by 90°. The current response of solution containing only supporting electrolyte was recorded before undertaking ecl measurements. Background current densities of 48 μA/cm^2 were measured at potential limits of −2.0 and +2.0 V.

Ecl spectra of $Mo_6Cl_{14}^{2-}$/acceptor and donor systems were recorded between 350 and 1100 nm by interfacing the electrochemical cell directly to the detection side of the emission spectrometer. The working electrode was located at the focal point of the collecting lens, and ecl was generated by a cyclic square wave (10 or 20 Hz) with potential limits appropriate to the acceptor or donor system under investigation.

The quantum yield for ecl is defined by the expression in eq 1, where I is the total ecl intensity (einsteins/s) over a finite period of time t and Q is the total faradaic charge collected in a single forward step. The

$$\phi_{ecl} = \int_0^t I\,dt/Q \qquad (1)$$

ecl yield is equivalent to the number of photons produced per electron transferred, and consequently ϕ_{ecl} can be determined by measuring the number of photons emanating from the electrode surface and the number of equivalents of electrogenerated species. The latter quantity can be measured coulometrically by monitoring the anodic and cathodic charge passed into solution during an ecl experiment. In regard to the former quantity, absolute ecl intensity measurements were performed by using an EG&G Electro-Optics 550-19 integrating sphere and an EG&G Model 550-1 photometer/radiometer equipped with an EG&G Model 550-2 multiprobe detector. A flat detector response between 450 and 1100 nm was achieved by fitting the multiprobe with a radiometric filter attachment provided by EG&G. Integration of the ecl intensity was accomplished with a Model 550-3 pulse integrator. Calibration of the integrating sphere was performed by EG&G Electro-Optics Division with photometric sources certified by the National Bureau of Standards.

Ecl yields were calculated with appropriate corrections for reflectivity of the electrode and non-faradaic contributions to the integrated current according to methods described by Bard.[60] Measurements of the ecl efficiency of $Ru(bpy)_3^{2+}$, which has been determined in several previous studies, were undertaken in an effort to allow us to check our experimental apparatus and procedure. An acetonitrile solution containing $Ru(bpy)_3^{2+}$ (μ = 0.1 M NBu_4ClO_4, $[Ru(bpy)_3^{2+}]$ = 3 mM) was prepared in the high-vacuum electrochemical cell, and ecl measurements were performed with the integrating sphere contained in a light-tight box. An ecl yield for a single run was determined from 20 measurements of the ecl intensity generated from a single triple-step potential sequence. The system was allowed to equilibrate 30 s between each pulse sequence. The overall yield calculated from five separate experiments was $\phi_{ecl}[Ru(bpy)_3^{2+}] = 0.046 \pm 0.004$. This value is in good agreement with the previously reported efficiency of 0.05 in CH_3CN at 25 °C.[25b,c]

Quantum yield measurements of acceptor and donor systems followed procedures similar to those described above. The cluster ion and electroactive reagent were contained in separate sample chargers. Prior to the addition of a given acceptor or donor to the working electrode compartment, the ecl yield of solutions containing only $Mo_6Cl_{14}^{2-}$ was determined from the average of a minimum of 10 pulses. Donor or acceptor was then introduced to solution, and ϕ_{ecl} was measured by a pulse sequence with potential limits appropriate to the system under investigation. This procedure permitted us to identify anomalous ecl measurements by monitoring the $Mo_6Cl_{14}^{2-}$ ecl efficiency. Error limits for $Mo_6Cl_{14}^{2-}$/donor and acceptor ϕ_{ecl} values in CH_3CN, determined from three experimental runs composed of 10 ecl intensity measurements, are given as the maximum deviation from the mean.

Accurate determinations of ϕ_{ecl} for acceptor and donor systems exhibiting the weakest ecl intensities were hampered by the low throughput of the integrating sphere. For these systems, the electrochemical cell was positioned directly on the face of the multiprobe detector. The ecl efficiencies of $Mo_6Cl_{14}^{2-}$/acceptor and donor systems were estimated with $Mo_6Cl_{14}^{2-}$ as a relative standard. In an experimental run, $Mo_6Cl_{14}^{2-}$ was initially added to solution, and the ecl yield was determined from a minimum of 20 intensity measurements. The electroactive organic reagent was then added to solution, and the ecl yield for the $Mo_6Cl_{14}^{2-}$/acceptor or donor system was recorded. In this manner, errors due to geometric positioning of the cell on the detector were minimized. Because the spectral distributions of the two experiments are identical, the ecl quantum yield of $Mo_6Cl_{14}^{2-}$/acceptor and donor system, ϕ_{ecl}, can be calculated directly from eq 2 where ϕ_{ecl^0} is the ecl efficiency of

$$\phi_{ecl} = \phi_{ecl^0}\frac{Q^0}{Q}\frac{I}{I^0} \qquad (2)$$

$Mo_6Cl_{14}^{2-}$ (μ = 0.1 M NBu_4ClO_4 in CH_3CN at 25 °C),[61] Q^0 and Q are the charges passed into solution, and I^0 and I are the measured integrated photon intensities of solution containing cluster and solution containing cluster and donor or acceptor, respectively. Ecl yields were calculated from the average of three experimental runs of 10 measurements; error limits of ϕ_{ecl}, measured by this method, were ±9% in CH_3CN.

Results

Electrochemical and quenching data are displayed in Table I for the aromatic amines, in Table II for the nitroaromatics,[62] and in Table III for the pyridinium ions employed as electroactive reagents in ecl studies. Reduction potentials of acceptors and donors were determined by cyclic voltammetry. All compounds exhibit reversible one-electron processes. Values of the ratio of anodic and cathodic current maxima i_c/i_a varied from 0.95 to 1.05, and plots of anodic and cathodic peak currents vs (scan rate)$^{1/2}$ were linear with a zero intercept. Anodic to cathodic peak separations (ΔE_p) of 90 mV for the three series of compounds were comparable to that measured for ferrocene (95 mV), thereby

(60) Keszthelyi, C. P.; Tokel-Takvoryan, N. E.; Bard, A. J. *Anal. Chem.* **1975**, *47*, 249–255.

(61) The ecl yield of $Mo_6Cl_{14}^{2-}$, determined from triple-step potential sequences, is 0.0045 ± 0.0009 in CH_3CN at 25 °C: Mussell, R. D.; Nocera, D. G., unpublished results.

(62) Owing to our inability to find nitroaromatics that are reduced at potentials less negative than *p*-dinitrobenzene, some aromatic quinones were employed for the reaction of $Mo_6Cl_{14}^{-}$ with negatively charged donors.

Table I. Reduction Potentials, Quenching Rate Constants,[a] and Ecl Quantum Yield Data[b] for Aromatic Amines Used in Ecl Studies[c]

acceptors (A)	$E_{1/2}$,[d] V	$\Delta G_{gs}°$,[e] V	k_q,[f] $M^{-1}\,s^{-1}$	ϕ_{ecl}[g]
1. phenothiazine	+0.21	−2.05	1.0×10^8	$<10^{-6}$ [h]
2. dimethoxydiphenylamine	+0.20	−2.04	1.1×10^8	$<10^{-6}$ [h]
3. 10-methylphenothiazine	+0.32	−2.16	2.3×10^7	6.0×10^{-4}
4. *N,N*-dimethyl-*p*-toluidine	+0.34	−2.18	2.0×10^7	6.6×10^{-4}
5. tri-*p*-tolylamine	+0.38	−2.22	8.0×10^6	3.1×10^{-3}
6. tris(4-bromophenyl)amine	+0.70	−2.54	5.8×10^5	2.5×10^{-2}

[a] Luminescence quenching of $Mo_6Cl_{14}^{2-}$ by neutral aromatic amines (A). [b] Ecl quantum yields for the reaction of $Mo_6Cl_{14}^{3-}$ with the aromatic amine cation radical (A^+). [c] All measurements were made in acetonitrile containing 0.1 M tetrabutylammonium perchlorate at 23 ± 2 °C. [d] As reduction potentials for the $A^{+/0}$ couple vs SCE. [e] Standard free energy change for the reaction of $Mo_6Cl_{14}^{3-}$ with A^+; $\Delta G_{gs}° = -[E_{1/2}(A^{+/0}) - E_{1/2}(Mo_6Cl_{14}^{2-/3-})]$. [f] Quenching rate constants determined from steady-state emission measurements. [g] Number of moles of photons produced per number of equivalents of $Mo_6Cl_{14}^{3-}$ or A^+. Error limits are ±8%. [h] Detection limit of the ecl quantum yield is 10^{-6}.

Table II. Reduction Potentials, Quenching Rate Constants,[a] and Ecl Quantum Yield Data[b] for Nitroaromatics and Aromatic Quinones Used in Ecl Studies

donors (D)	$E_{1/2}$,[d] V	$\Delta G_{gs}°$,[e] V	k_q,[f] $M^{-1}\,s^{-1}$	ϕ_{ecl}[g]
1. *p*-benzoquinone	−0.55	−2.11	2.3×10^6	$<10^{-6}$ [h]
2. 2,6-dimethyl-*p*-benzoquinone	−0.72	−2.28	4.5×10^5	4.1×10^{-5}
3. *p*-dinitrobenzene	−0.75	−2.31	1.1×10^5	3.5×10^{-4}
4. *o*-dinitrobenzene	−0.91	−2.47	3.9×10^3	1.1×10^{-3}
5. *p*-nitrobenzaldehyde	−0.92	−2.48	5.8×10^4	1.4×10^{-3}
6. *m*-nitrobenzaldehyde	−1.09	−2.65	5.6×10^4	2.4×10^{-3}
7. 1-chloro-4-nitrobenzene	−1.13	−2.69	3.7×10^3	1.5×10^{-3}
8. 5-nitro-*m*-xylene	−1.26	−2.82	1.9×10^3	9.5×10^{-4}
9. 3-nitro-*o*-xylene	−1.39	−2.95	1.2×10^3	6.8×10^{-4}

[a] Luminescence quenching of $Mo_6Cl_{14}^{2-}$ by neutral donors (D). [b] Ecl quantum yields for the reaction of $Mo_6Cl_{14}^{-}$ with reduced donors (D^-). [c] All measurements were made in acetonitrile containing 0.1 M tetrabutylammonium perchlorate at 23 ± 2 °C. [d] As reduction potentials for the $D^{0/-}$ couple vs SCE. [e] Standard free energy change for the reaction of $Mo_6Cl_{14}^{-}$ with D^-; $\Delta G_{gs}° = -[E_{1/2}(Mo_6Cl_{14}^{-/2-}) - E_{1/2}(D^{0/-})]$. [f] Quenching rate constants determined from steady-state emission measurements. [g] Number of moles of photons produced per number of equivalents of $Mo_6Cl_{14}^{-}$ or D^-. Error limits are ±10%. [h] Detection limit of the ecl quantum yield is 10^{-6}.

Table III. Reduction Potentials, Quenching Rate Constants,[a] and Ecl Quantum Yield Data[b] for Pyridinium Salts Used in Ecl Studies[c]

donors (D^+)[d]	$E_{1/2}$,[e] V	$\Delta G_{gs}°$,[f] V	k_q,[g] $M^{-1}\,s^{-1}$	ϕ_{ecl}[h]
1. 4-cyano-*N*-benzylpyridinium	−0.69	−2.25	2.2×10^7	2.4×10^{-3}
2. 4-cyano-*N*-methylpyridinium	−0.74	−2.30	4.4×10^5	6.1×10^{-3}
3. 4-carbethoxy-*N*-benzyl-pyridinium	−0.84	−2.40	4.9×10^4	1.2×10^{-2}
4. 4-carbethoxy-*N*-methyl-pyridinium	−0.88	−2.44	2.6×10^4	1.2×10^{-2}
5. 4-amido-*N*-benzylpyridinium	−0.96	−2.52	1.8×10^4	1.3×10^{-2}
6. 4-amido-*N*-methylpyridinium	−1.02	−2.58	1.2×10^4	1.5×10^{-2}

[a] Luminescence quenching of $Mo_6Cl_{14}^{2-}$ by pyridinium ions (D^+). [b] Ecl quantum yields for the reaction of $Mo_6Cl_{14}^{-}$ with one-electron-reduced pyridinium ion (D). [c] All measurements were made in acetonitrile contalning 0.1 M tetrabutylammonium perchlorate at 23 ± 2 °C. [d] Hexafluorophosphate salts. [e] As reduction potentials for the $D^{+/0}$ couple vs SCE. [f] Standard free energy change for the reaction of $Mo_6Cl_{14}^{-}$ with D; $\Delta G_{gs}° = -[E_{1/2}(Mo_6Cl_{14}^{-/2-}) - E_{1/2}(D^{+/0})]$. [g] Quenching rate constants determined from steady-state emission measurements. [h] Numbers of moles of photons produced per number of equivalents of $Mo_6Cl_{14}^{-}$ or D. Error limits are ±12%.

establishing that deviations of ΔE_p from the theoretical value of 59 mV are due primarily to uncompensated cell resistance.[63] Rate constants for the quenching of $Mo_6Cl_{14}^{2-}$ luminescence in CH_3CN (μ = 0.1 M NBu_4ClO_4 at 25 °C) were deduced from classical Stern–Volmer analysis of the emission intensity. All Stern–Volmer plots were linear over a quencher concentration range of 1–100 mM and k_q's were calculated from Stern–Volmer constants with $\tau_0(Mo_6Cl_{14}^{2-*}) = 180$ μs in CH_3CN (μ = 0.1 M NBu_4ClO_4 at 25 °C). The electrochemical and quenching properties listed in Tables I and II are in good agreement with our previous measurements[56] of these compounds in CH_2Cl_2.

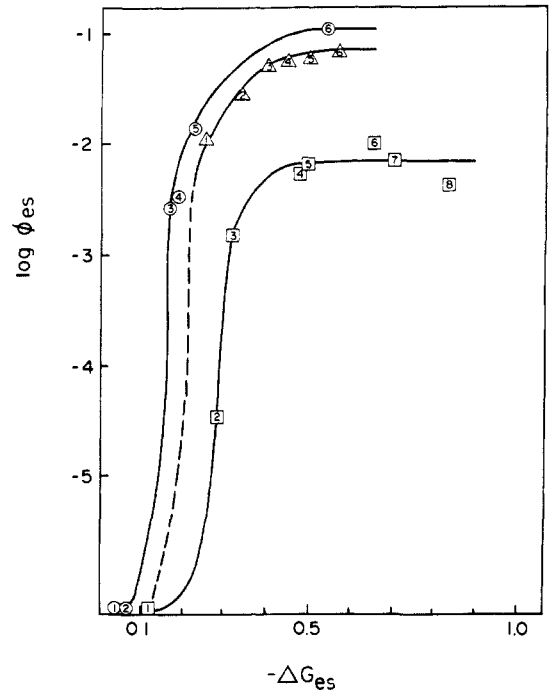

Figure 1. Plot of log ϕ_{es} versus ΔG_{es} for the electron-transfer annihilation reactions of the $Mo_6Cl_{14}^{3-}/A^+$ (○), $Mo_6Cl_{14}^{-}/D$ (△), and $Mo_6Cl_{14}^{-}/D^-$ (□) systems. The numbering scheme is defined in Tables I–III. The standard free energy change for the excited-state reaction pathway was evaluated as described in footnote 66.

Owing to the insolubility of the pyridinium salts in CH_2Cl_2 and to our desire to perform all ecl experiments in a common solvent, ecl studies of $Mo_6Cl_{14}^{2-}$/acceptor and donor systems were carried out in CH_3CN. Since $D^{0/-}$ and $D^{+/0}$ reduction potentials are positive of the $Mo_6Cl_{14}^{2-/3-}$ couple and $A^{+/0}$ reduction potentials are negative of the $Mo_6Cl_{14}^{-/2-}$ couple, the electron-transfer reactions in eq 3 and 4 can cleanly be established by standard

$$Mo_6Cl_{14}^{3-} + A^+ \rightarrow Mo_6Cl_{14}^{2-*} + A \quad (3a)$$

$$Mo_6Cl_{14}^{3-} + A^+ \rightarrow Mo_6Cl_{14}^{2-} + A \quad (3b)$$

$$Mo_6Cl_{14}^{-} + \begin{pmatrix} D^- \\ D \end{pmatrix} \rightarrow Mo_6Cl_{14}^{2-*} + \begin{pmatrix} D \\ D^+ \end{pmatrix} \quad (4a)$$

$$Mo_6Cl_{14}^{-} + \begin{pmatrix} D^- \\ D \end{pmatrix} \rightarrow Mo_6Cl_{14}^{2-} + \begin{pmatrix} D \\ D^+ \end{pmatrix} \quad (4b)$$

electrochemical techniques.[64] Chemiluminescence from the $Mo_6Cl_{14}^{2-}$/donor and acceptor systems is observed only when the potential applied to the working Pt electrode is stepped into the oxidation–reduction waves of the electroactive species. Tables I–III list the free energy changes and the ecl quantum yields, ϕ_{ecl}, for reactions 3 and 4. Ecl quantum efficiencies were determined by dividing the number of einsteins emanating from the electrode surface by the number of equivalents of electrons used to generate the oxidant or reductant (i.e., the integrated anodic or cathodic charge passed into solution). As evidenced by the relatively small quenching rate constants listed in Tables I–III, acceptors and donors are inefficient quenchers of $Mo_6Cl_{14}^{2-}$ luminescence, and therefore the measured ecl intensities are not attenuated by the presence of acceptor or donor.[65] Additionally, for systems ex-

(63) Cyclic voltammetry experiments were performed at scan rates of 200 mV s^{-1}, and no *iR* compensation was used. When the scan rate is slowed to 50 mV s^{-1} and *iR* compensation employed, cyclic voltammograms of all acceptors and donors exhibit anodic to cathodic peak separations of 75 mV.

(64) Faulkner, L. R.; Bard, A. J. *Electroanal. Chem.* **1977**, *10*, 1–95.

hibiting ecl, the spectrum is identical with the emission spectrum of $Mo_6Cl_{14}^{2-}$ in CH_3CN. The absence of acceptor or donor luminescence is consistent with spectroscopic data, which reveals that population of the lowest energy electronic excited state of the compounds collected in Tables I–III is an energetically unfavorable process.[66]

The excited-state yield, ϕ_{es}, is related to the ecl quantum efficiency by eq 5 where ϕ_e is the emission quantum yield. Since

$$\phi_{ecl} = \phi_{es}\phi_e \quad (5)$$

ϕ_e is an intrinsic property of the luminescent excited state, it is ϕ_{es} that is fundamentally descriptive of the efficiency of the chemiluminescent process. Figure 1 shows a plot of ϕ_{es} vs the free energy driving force of the excited-state reactions ($\Delta G_{es}^\circ = \Delta G_{gs}^\circ$ + 2.0 V) for acceptors and donors listed in Tables I–III.[67] The excited-state yields were calculated with $\phi_e = 0.19$ for $Mo_6Cl_{14}^{2-}$ in CH_3CN at 25 °C.

Discussion

Electronically excited $Mo_6Cl_{14}^{2-}$ ion is produced by the simple electron-transfer reactions of the electrochemically generated $Mo_6Cl_{14}^{-}$ and $Mo_6Cl_{14}^{3-}$ ions with electroactive donors and acceptors, respectively. The chemiluminescent reactivity of the oxidized and reduced forms of $Mo_6Cl_{14}^{2-}$ can neatly be accommodated in terms of the hexanuclear cluster's electronic structure. In recent years, a detailed picture of the frontier molecular orbitals of the $M_6X_{14}^{2-}$ ions has been developed. Extended Hückel[68] and SCF-Xα–SW[69] calculations predict the HOMO and LUMO to be primarily metal in character and to possess molecular symmetries e_g and a_{2g}, respectively (vide infra). These results are consistent with spectroscopic studies, which suggest that the luminescence of the $M_6X_{14}^{2-}$ ions originates from an excited state localized on the metal core.[70] Additionally, magnetic measurements establish a diamagnetic ground state for $M_6X_{14}^{2-}$ ions, and the oxidized $M_6X_{14}^{-}$ cluster ions display an axial EPR signal, which can be attributed to a tetragonally distorted metal core resulting from the single-electron occupancy of the e_g level.[71] On the basis of these spectroscopic and theoretical results, the ecl chemistry of the $Mo_6Cl_{14}^{-}$ and $Mo_6Cl_{14}^{3-}$ ions is described by the molecular orbital representation depicted in Figure 2. For the $Mo_6Cl_{14}^{3-}/A^+$ series, the a_{2g} orbital is occupied prior to annihilation and, therefore, transfer of an electron from the e_g orbital to the appropriate acceptor level will yield an electronically excited cluster. Directly opposing this excited-state pathway is removal of the electron from the a_{2g} orbital to afford a ground-state cluster ion. In the case of the $Mo_6Cl_{14}^{-}/D^-$ and D systems, transfer of an electron from the donor level to the cluster's a_{2g} orbital directly yields an electronically excited ion whereas exchange to the e_g orbital brings the cluster ion to its ground state.

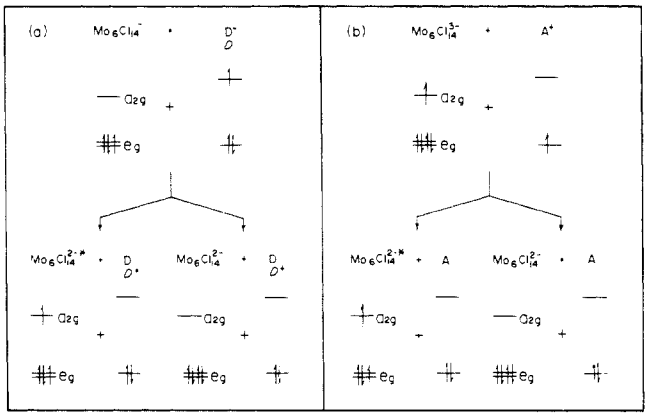

Figure 2. Molecular orbital description for competitive electron transfer to give either ground- or excited-state $Mo_6Cl_{14}^{2-}$ by the reaction of (a) $Mo_6Cl_{14}^{3-}$ with oxidized aromatic amines (A^+) and (b) $Mo_6Cl_{14}^{-}$ with reduced nitroaromatics (D^-) or pyridinium ions (D). Production of electronically excited acceptors and donors is an energetically unfavorable process.

It is evident from Figure 2 that cl is directly competitive with the ground-state reaction. Specifically, the yield for excited-state production is given by eq 6 where k_{es} and k_{gs} are the rate constants

$$\phi_{es} = k_{es}/k_{gs}/(k_{es}/k_{gs} + 1) \quad (6)$$

for electron transfer to produce excited-state and ground-state products, respectively. The functional dependence of ϕ_{es} on the driving force of the electron-transfer reaction is similar for the three series (see Figure 1). Namely, the $Mo_6Cl_{14}^{2-}$/acceptor and donor systems possess a free energy threshold for ecl. At energies negative of threshold, ϕ_{es} rapidly increases and approaches a limiting value with increasing exergonicity. Substitution of the asymptotically limiting values of the excited-state yields for the $Mo_6Cl_{14}^{3-}/A^+$, $Mo_6Cl_{14}^{-}/D$, and $Mo_6Cl_{14}^{-}/D^-$ systems into eq 6 gives k_{es}/k_{gs} ratios of 0.15, 0.083, and 0.013, respectively. These values clearly establish that the excited-state reaction pathway is kinetically competitive with the ground-state reaction, even though the latter is favored thermodynamically by 2.0 V. This kinetic enhancement of the excited-state pathway may be understood within the context of an electron-transfer model for cl, first proposed by Marcus,[72] in which electron transfer to produce ground-state products is so exergonic that it lies in the inverted region and therefore is inhibited. In contrast, the modest exergonicity of the exchange reaction to produce excited-state products occurs in the normal region, and consequently electron transfer proceeds at relatively rapid rates. More quantitatively, the ratio of the excited-state and ground-state rates is given by[73] eq 7 where λ_{es} and λ_{gs} are the reorganizational energies for excited-state and ground-state reactions. This rate expression assumes that electron transfer is adiabatic and occurs at a reaction distance of closest contact (i.e., $r_{ij} = a_i + a_j$ where a_i and a_j are the radii of the two reactants and r_{ij} is the distance between their centers). The reorganizational energy for electron transfer com-

$$2.3RT \log \frac{k_{es}}{k_{gs}} = \tfrac{1}{4}(\lambda_{gs} - \lambda_{es}) + \tfrac{1}{2}(\Delta G_{gs}^\circ - \Delta G_{es}^\circ) + \tfrac{1}{4}\left(\frac{(\Delta G_{gs}^\circ)^2}{\lambda_{gs}} - \frac{(\Delta G_{es}^\circ)^2}{\lambda_{es}}\right) \quad (7)$$

(65) The concentration profiles of electrogenerated intermediates do not significantly overlap in an ecl step experiment,[64] and hence $Mo_6Cl_{14}^{2-*}$ should not be quenched by the electrogenerated cluster or electroactive organic reactants. Even when the production of the electroactive organic reactant was doubled, significant quenching of the ecl was not observed.

(66) The lowest excited-state energies for donors and acceptors used in ecl studies are the following: 2,6-dimethyl-*p*-benzoquinone, E_T = 2.32 V (Trommsdorff, H. P. *J. Chem. Phys.* **1972**, *56*, 5358–5372); *p*-dinitrobenzene, E_T = 2.54 V (Brown, R. G.; Harriman, A.; Harris, L. *J. Chem. Soc., Faraday Trans. 2*, **1978**, *74*, 1193–1199); *o*-dinitrobenzene, E_T = 2.55 V, and phenothiazine, E_T = 2.62 V (Alkaitis, S. A.; Gratzel, M.; Henglein, A. *Ber. Bunsenges, Phys. Chem.* **1975**, *79*, 541–546); 10-methylphenothiazine, E_T = 2.66 V (Rothenberger, G.; Infelta, P. P.; Gratzel, M. *J. Phys. Chem.* **1979**, *83*, 1871–1876); tri-*p*-tolylamine, E_T = 3.0 V (Zachariasse, K. A. Ph.D. Thesis, Free University Press: Amsterdam, 1972); tris(4-bromophenyl)amine, $E_T \geq$ 3.1 V (Terenen, A.; Ermolaev, V. *Sov. Phys.—Dokl. (Engl. Transl.)* **1962**, *6*, 600–602).

(67) The standard free energy change, ΔG_{es}, of the excited-state electron-transfer pathway (reactions 3a and 4a) was calculated from $\Delta G_{es}^\circ = \Delta G_{es}^\circ - \Delta G_{ES}$ where ΔG_{ES} is the free energy content of the $Mo_6Cl_{14}^{2-}$ excited state over the ground state and ΔG_{gs}° is the standard free-energy change of the ground-state reaction pathway. ΔG_{ES} can be estimated from the energy of 0,0 transition ($E_{0,0}$ = 1.9 eV) with corrections for entropic contributions ($T\Delta S$ = 0.1 V): Faulkner, L. R.; Tachikawa, H.; Bard, A. J. *J. Am. Chem. Soc.* **1972**, *94*, 691–699).

(68) Hughbanks, T.; Hoffman, R. *J. Am. Chem. Soc.* **1983**, *105*, 1150–1162.

(69) (a) Seifert, G.; Grossman, G.; Muller, H. *J. Mol. Struct.* **1980**, *64*, 93–102. (b) Tyler, D. R., University of Oregon, personal communication, 1986.

(70) Zietlow, T. C.; Nocera, D. G.; Gray, H. B. *Inorg. Chem.* **1986**, *25*, 1351–1353.

(71) Maverick, A. W.; Najdzionek, J. S.; MacKenzie, D.; Nocera, D. G.; Gray, H. B. *J. Am. Chem. Soc.* **1983**, *105*, 1878–1882.

(72) Marcus, R. A. *J. Chem. Phys.* **1965**, *43*, 2654–2657.

(73) Marcus, R. A. *Annu. Rev. Phys. Chem.* **1964**, *15*, 155–196.

prises inner- and outer-sphere contributions ($\lambda = \lambda_i + \lambda_o$). The outer-sphere reorganizational parameter in a dielectric continuum is[74] given in eq 8 where ϵ_s and ϵ_{op} are the static and optical dielectric

$$\lambda_o = (\Delta e)^2\left[\frac{1}{2a_i} + \frac{1}{2a_j} - \frac{1}{r_{ij}}\right]\left[\frac{1}{\epsilon_{op}} - \frac{1}{\epsilon_s}\right] \quad (8)$$

constants of the solvent. The structural similarities of the acceptors and donors listed in Tables I–III are manifested in a nearly constant value of $\lambda_o = 0.86 \pm 0.05$ eV for reactions 3 and 4.[75] The inner-sphere reorganizational parameter depends on differences in equilibrium bond lengths and angles between reactants and products. In regard to acceptors and donors, calculations using measured self-exchange rate constants for several aromatic amines and nitroaromatics[76] establish that the overall λ_i's associated with the electron-transfer reactions of these compounds are <0.05 eV.[77] For cluster reactants, self-exchange rate constants of the $Mo_6Cl_{14}^{2-}$ ion are not known, but as Hush has shown,[78] λ_i can be estimated from the emission bandwidth of solid $Mo_6Cl_{14}^{2-}$ at room temperature. When the experimentally determined half-width of 3700 cm^{-1} and an excited state energy of 1.9 V are used, λ_i is calculated to be 0.70 V. Crystal structure[79] and EPR data[71,79] of $M_6X_{14}^-$ ions reveal that the oxidized cluster ion is structurally similar to $Mo_6Cl_{14}^{2-}$, and therefore little reorganization will result from exchange of electrons to or from the e_g orbital. On this basis, the reorganizational energy of 0.70 eV appears to be primarily associated with population of the a_{2g} molecular orbital. Consequently, although λ_o for the ground- and excited-state reactions is nearly equivalent, electron-exchange reactions involving the a_{2g} orbital of the cluster will exhibit $\lambda_i \sim 0.70$ V, whereas exchange reactions involving the e_g orbital will result in a negligible inner-sphere reorganizational energy.

With the appropriate values of λ_{es} and λ_{gs}, k_{es}/k_{gs} can now be evaluated for reactions 3 and 4. For purposes of comparison between the three series, we focus on the electron-transfer reactions of the $Mo_6Cl_{14}^{3-}$/tris(4-bromophenyl)amine cation (BPA; $\Delta G_{es}° = -0.54$ V, $\Delta G_{gs}° = -2.54$ V), the $Mo_6Cl_{14}^{-}$/*p*-nitrobenzaldehyde anion (NBA; $\Delta G_{es}° = -0.48$ V, $\Delta G_{gs}° = -2.48$ V), and $Mo_6Cl_{14}^{-}$/4-cyano-*N*-methylpyridinium (CMP; $\Delta G_{es}° = -0.30$ V, $\Delta G_{gs}° = -2.30$ V) because these systems exhibit asymptotically limiting values of ϕ_{es} for their respective series. Using eq 7, we calculate values of $k_{es}/k_{gs} = 1.3 \times 10^2$, 5.4×10^6, and 6.4×10^8 for the $Mo_6Cl_{14}^{3-}$/BPA^+, $Mo_6Cl_{14}^{-}$/CMP, and $Mo_6Cl_{14}^{-}$/NBA^- systems, respectively. These values are 10^3–10^{10} greater than those determined from the measured excited-state yields listed in Tables I–III [$k_{es}/k_{gs}(Mo_6Cl_{14}^{3-}/BPA^+) = 0.15$; $k_{es}/k_{gs}(Mo_6Cl_{14}^{-}/CMP) = 0.033$; $k_{es}/k_{gs}(Mo_6Cl_{14}^{-}/NBA^-) = 0.0072$]. This striking discrepancy between the theoretically predicted and experimentally measured rates of the ground- and excited-state electron transfer is not specific to $Mo_6Cl_{14}^{2-}$ ecl but, as mentioned above, is typical of many inorganic transition-metal complexes displaying chemiluminescent reactivity.[25] Deviations from inverted-region behavior have been attributed to a variety of reasons including decomposition of the reactants before annihilation and to a failure of the Marcus model in the inverted region owing to the presence of competitive reaction pathways such as H-atom transfer or the formation of nonemissive excited-state products.[3a,6a,34] None of these reasons, however, satisfactorily explain the results of $Mo_6Cl_{14}^{2-}$ ecl. For example, invoking a competitive electron-transfer pathway to rationalize the low yields of systems in this study is not reasonable because acceptors and donors were judiciously chosen such that population of their excited states is an energetically unfavorable process. In addition, we can explicitly rule out deviations from theoretical predictions resulting from the chemical instability of the reactants on the basis of the electrochemical reversibility of the cluster and electroactive organic reactants. Thus, differences in calculated and observed rates of the $Mo_6Cl_{14}^{2-}$/acceptor and donor systems bear directly, by design, on the mechanistic features of electron transfer at high exergonicities.

A crucial mechanistic feature of reactions 3 and 4 not explicitly accounted for by the Marcus expressions used to derive eq 7 is that cl results from bimolecular electron transfer, which can occur over a range of distances.[80,81] The overall rate constant is a harmonic mean of the diffusion-limited rate, k_{diff}, and the activated rate, k_{act}, as shown in eq 9, and as Marcus and Siders have

$$1/k_{obsd} = 1/k_{diff} + 1/k_{act} \quad (9)$$

discussed,[80] under steady-state conditions k_{act} and k_{diff} are approximated by[82–84] eq 10 and 11. In these expressions, $k(r)$ is

$$k_{diff} = \frac{4\pi ND}{1000} \Big/ \int_\sigma^\infty g_e(r)\, r^{-2}\, dr \quad (10)$$

$$k_{act} = \frac{4\pi N}{1000}\int_\sigma^\infty g_e(r)\, k(r)\, r^2\, dr \quad (11)$$

the unique unimolecular rate of reaction between reactants at a center-to-center separation distance r, D is the sum of the reactants' diffusion coefficients, and $g_e(r)$ is the equilibrium pair distribution function given in eq 12 where $U(r)$ represents the intermolecular

$$g_e(r) = \exp[-U(r)/k_BT] \quad (12)$$

potential between the reactants. Typically, $U(r)$ is described by a Debye–Hückel approximation; therefore, $g_e(r) = 1$ for reactions in which one of the species is neutral, and eq 10 reduces to the more familiar expression $k_{diff} = 4\pi DN\sigma/1000$. For nonadiabatic electron transfer, $k(r)$ is given by eq 13 and 14 where β is a

$$k(r) = \left[\frac{2H_{AB}^2}{h}\right]\left[\frac{\pi^3}{\lambda k_BT}\right]^{1/2}\exp\left[\frac{-(\lambda + \Delta G°)^2}{4\lambda k_BT}\right] \quad (13)$$

$$H_{AB} = H_{AB}^0 \exp[-\beta(r - \sigma)] \quad (14)$$

constant and H_{AB} is the electronic coupling element.[85] Typical electron-transfer reactions of transition-metal complexes in homogeneous solution are characterized by values of β ranging from 1.2 to 1.6 $Å^{-1}$ and H_{AB}^0 ranging from 20 to 500 cal.[86] Thus, eq 9–14 permit us to examine, with the previously determined values of λ and the appropriate values of β and H_{AB}^0, the distance dependence of the observed bimolecular rate constants of the excited-state and ground-state electron-transfer annihilation reactions of the $Mo_6Cl_{14}^{2-}$/acceptor and donor systems.

The distance dependence of the excited-state and ground-state pathways is most easily illustrated by differentially solving the integrals in eq 10 and 11 between r and $r + \delta r$ for reaction separation distances from an arbitrarily large value of 20 Å to a closest contact distance of 9.3 Å.[87] We initially focus on the

(74) Marcus, R. A. *J. Chem. Phys.* **1956**, *24*, 966–978.
(75) We have calculated the radii equivalent to the sphere of equal volume, $a = {}^1/_2(d_1d_2d_3)^{1/3}$, for all acceptors and donors used in our ecl studies. d_i represents the van der Waals diameter along the molecular axes.
(76) Kowert, B. A.; Marcoux, L.; Bard, A. J. *J. Am. Chem. Soc.* **1972**, *94*, 5538–5550.
(77) λ values were determined from the Marcus self-exchange relation $k = Z\exp(-\lambda/4RT)$ with $Z = 10^{11}$ s^{-1} and the measured self-exchange rate constants for k.
(78) Hush, N. S. *Prog. Inorg. Chem.* **1967**, *8*, 391–444.
(79) Zietlow, T. C.; Schaefer, W. P.; Sadeghi, B.; Nocera, D. G.; Gray, H. B. *Inorg. Chem.* **1986**, *25*, 2198–2201.
(80) Marcus, R. A.; Siders, P. *J. Phys. Chem.* **1982**, *86*, 622–630.
(81) (a) Brunschwig, B. S.; Ehrenson, S.; Sutin, N. *J. Am. Chem. Soc.* **1984**, *106*, 6858–6859. (b) Isied, S. S.; Vassilian, A.; Wishart, J. F.; Creutz, C.; Schwarz, H. A.; Sutin, N. *J. Am. Chem. Soc.* **1988**, *110*, 635–637.
(82) Marcus, R. A. *Discuss. Faraday Soc.* **1960**, *29*, 129–131.
(83) Noyes, R. M. *Prog. React. Kinet.* **1961**, *1*, 129–160.
(84) Debye, P. *Trans. Electrochem. Soc.* **1942**, *82*, 265–272.
(85) Hopfield, J. J. *Proc. Natl. Acad. Sci. U.S.A.* **1974**, *71*, 3640–3644.
(86) Sutin, N. *Acc. Chem. Res.* **1982**, *15*, 275–282.
(87) (a) The integrand in eq 11 for given r greater then the closest contact distance of 9.3 Å can be approximated by $k_{act} = (4\pi N/1000)g_e(r)\, k(r)\, r^2\, \delta r$ (M^{-1} s^{-1}), where $\delta r = 0.8$ Å.[82b] (b) Sutin, N.; Brunschwig, B. S. *ACS Symp. Ser.* **1982**, *No.* **198**, 105–125.

results of the $Mo_6Cl_{14}^{2-}$/pyridinium series because calculations for the electron-transfer annihilation reactions of this system are simplified by the fact that $g_e(r) = 1$. Figure 3 shows a plot of the excited-state and ground-state differential rate constants ($k_{es,difn}$ and $k_{gs,difn}$, respectively) as a function of r for the electron-transfer reactions of $Mo_6Cl_{14}^-$ with CMP (eq 15 and 16). Equations 10

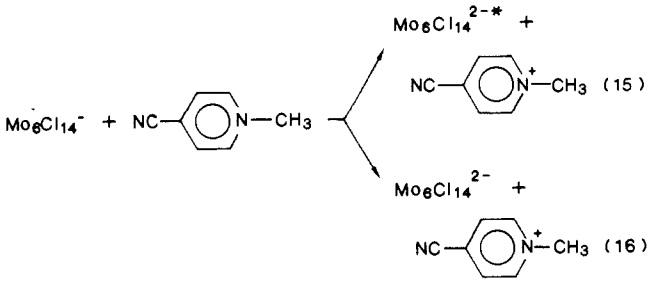

and 11 were evaluated by use of an encounter distance, σ, of 9.3 Å, a diffusion coefficient of 5×10^{-6} cm^2 s^{-1}, $H_{AB}^0 = 200$ cal, and $\beta = 1.2$ Å^{-1}. The large value of $k_{es,difn}$ ($=k_{gs,difn} \times 10^6$) at $r = \sigma$ clearly establishes that formation of electronically excited $Mo_6Cl_{14}^{2-}$ is preferred for electron transfer occurring at a separation distance of closest approach. In this regard, the results of eq 10 and 11 at $r = \sigma$ are consistent with those obtained with eq 7. With increasing distance, however, $k_{es,difn}$ and $k_{gs,difn}$ exhibit striking differences in their functional dependences on r. This contrasting behavior of $k_{es,difn}$ and $k_{gs,difn}$ is derived from opposing contributions of λ_o to the electron-transfer rate in the normal and inverted region. As described above, the electron-transfer rate is related to the separation distance via the electronic coupling element and outer-sphere reorganizational energy (λ_i is independent of r). From eq 8 and 14, an increase in r causes λ_o to increase and H_{AB} to decrease in magnitude. For reactions in the normal region (i.e., $-\Delta G° < \lambda$), as is reaction 15, an increase in λ_o raises the activation barrier to electron transfer, and the rate becomes attenuated. Couple this effect with an abatement in rate due to decreasing H_{AB} and, as observed in Figure 3, an increase in r is accompanied by a steady diminution in $k_{es,difn}$. Conversely, although an exponential decrease of H_{AB} with r contributes to a decrease of the electron-transfer rate in the inverted region (i.e., $-\Delta G° > \lambda$), it follows directly from eq 13 that the increase of λ_o causes an enhancement of the electron-transfer rate in the inverted region. These opposing effects of H_{AB} and λ_o on the electron-transfer rate are reflected in a maximum of $k_{gs,difn}$ at $r = 15$ Å. The disparate behavior of differential excited-state and ground-state rates with separation distance has interesting implications for the chemiluminescent reactivity of the $Mo_6Cl_{14}^{2-}$/CMP^+ system. As Figure 3 clearly illustrates, the contribution of the ground-state pathway to the overall rate comes from $r > \sigma$, while most of the contribution for excited-state production comes from $r \sim \sigma$. Thus, the appreciable values of $k_{gs,difn}$ at $r > \sigma$ suggest that electron transfer to yield ground-state products is competitive with excited-state production.

The integral (or overall) excited-state (k_{es}) and ground-state (k_{gs}) rates are explicitly related to the experimentally measured chemiluminescence yields by eq 6. Accordingly, the reaction distance for electron transfer can be determined by integrating eq 10 and 11 from $r = \infty$ to a value of r that yields a k_{es}/k_{gs} ratio commensurate with that calculated from the observed chemiluminescence yields. For the $Mo_6Cl_{14}^-$/CMP annihilation reaction, an observed k_{es}/k_{gs} ratio of 0.033 yields an electron-transfer reaction distance of 13 Å. This result clearly implies that approach of the electrogenerated reactants to a distance of closest approach ($\sigma = 9.3$ Å) is impeded. Recent studies of outer-sphere electron-transfer reactions of inorganic metal complexes in nonaqueous solution have demonstrated that ion pairing decreases electron-transfer rates by increasing the electron-transfer distance.[88-90]

When the relatively high ionic strengths used in our ecl experiments are considered, ion association between the supporting electrolyte and charged reactants is likely, and in this case, reaction at short distances will be inhibited. Indeed, we have observed a marked dependence of the ecl intensity on the nature of supporting electrolyte. More detailed investigations aimed at assessing the influence of solvent and ion association on ecl will be reported in a separate study. Thus, our calculations indicate that electron transfer between $Mo_6Cl_{14}^-$ and CMP occurs at reasonably rapid rates over large separation distances to produce $Mo_6Cl_{14}^{2-}$ ion.

The above analysis not only accounts for ϕ_{es} values of less than unity, but it also qualitatively explains the general dependence of ϕ_{es} on $\Delta G°$ for the acceptor and donor systems depicted in Figure 1. Differential ground- and excited-state rates obtained by numerically solving eq 10 and 11 for the remaining pyridinium systems are summarized in Figure 4. We have also included in Figure 4 calculations performed for hypothetical pyridinium systems with exergonicities below and near the ecl threshold free energy; these results are indicated by dashed lines. (Electron-transfer annihilation reactions between $Mo_6Cl_{14}^-$ and pyridinium radicals with driving forces less than the ecl threshold free energy, inferred from extrapolation of the data shown in Figure 1, were not investigated, owing to our inability to find pyridinium reagents meeting the necessary criteria required of electroactive reagents for ecl studies.) Annihilation reactions possessing driving forces below the ecl threshold energy exhibit comparable excited- and ground-state differential rate constants at distances near close contact. Consequently, the ground-state electron-transfer pathway is dominant over all r and, therefore, $k_{gs} \gg k_{es}$ and $\phi_{es} \ll 1$. As the driving force of the annihilation reaction increases, electron transfer to yield excited-state products becomes competitive with the ground-state reaction pathway as evidenced by the attenuation of $k_{gs,difn}$ and concomitant increase in $k_{es,difn}$ over all r. At large exergonicities, electron exchange to produce an electronically excited cluster ion will predominate, and ϕ_{es} should be unity. That ϕ_{es} appears to approach an asymptotically limiting value of less than unity (Figure 1) suggests that the ground-state reaction rate is not attenuated to the extent predicted by eq 13. We believe this anomalous behavior is nested in the fact that eq 13 is a classical expression and does not include nuclear tunneling effects, which can significantly enhance the rate of electron transfer for reactions with large exergonicities.[39a,80,81b]

Calculations of the integral rates k_{es} and k_{gs} for the $Mo_6Cl_{14}^{2-}$/A and D systems are similar to those of the $Mo_6Cl_{14}^{2-}$/D^+ system; however, the equilibrium pair distribution function must be evaluated for the former series. Parallel to the results described above, although formation of excited-state $Mo_6Cl_{14}^{2-}$ is favored for electron exchange between proximate reactants, the long-distance electron-transfer channel yielding ground-state products contributes significantly to $Mo_6Cl_{14}^{3-}$/A^+ and $Mo_6Cl_{14}^-$/D^- annihilation. Solving eq 10 and 11 with the experimentally measured yields of the $Mo_6Cl_{14}^{3-}$/A^+ and $Mo_6Cl_{14}^-$/D^- systems listed in Tables I and II gives reaction separation distances ranging from 11 to 18 Å.

Evaluation of eq 10 and 11 for the $Mo_6Cl_{14}^{2-}$/acceptor and donor systems necessarily relies on estimates of H_{AB}^0 and β. It is satisfying that the general conclusions derived from Figures 3 and 4 do not significantly depend on these estimates. Specifically, the relative dependence of the ground- and excited-state rates vary only marginally over the rather large interval 0.8 Å$^{-1} < \beta < 1.8$ Å^{-1}, which includes any reasonable value of β for the reactions of the type described in our ecl studies. Furthermore, H_{AB}^0 is a constant, and therefore the excited- and ground-state electron-transfer pathways exhibit a parallel dependence on the electronic coupling element. This result is predicated on our tacit assumption that H_{AB}^0 is similar for the ground- and excited-state pathways. Recently, the effect of disparate values of the electronic coupling element on chemiluminescent reactivity has been addressed for

(88) (a) Borchardt, D.; Pool, K.; Wherland, S. *Inorg. Chem.* **1982**, *21*, 93-97. (b) Nielson, R. M.; Wherland, S. *Inorg. Chem.* **1984**, *23*, 1338-1344. (c) Borchardt, D.; Wherland, S. *Inorg. Chem.* **1984**, *23*, 2537-2542. (d) Nielson, R. M.; Wherland, S. *Inorg. Chem.* **1986**, *25*, 2437-2440.

(89) Kjaer, A. M.; Ulstrup, J. *Inorg. Chem.* **1986**, *25*, 644-651.

(90) Truong, T. B. *Pure Appl. Chem.* **1986**, *58*, 1279-1284.

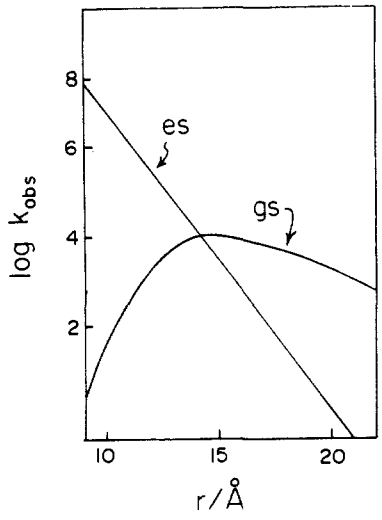

Figure 3. Distance dependence of the differential bimolecular rate constant for the excited-state (es) and ground-state (gs) electron-transfer channels for the reaction between $Mo_6Cl_{14}^-$ and one-electron-reduced 4-cyano-*N*-methylpyridinium (CMP), calculated by solving eq 8–14 between r and $r + \delta r$ with $\beta = 1.2$ Å^{-1} and $H_{AB}^0 = 200$ cal.

annihilation reactions involving transition-metal polypyridyl complexes.[22] Although the magnitudes of these effects have not explicitly been evaluated for metal polypyridyl complexes or for that matter any chemiluminescent system to date, the discrepancies in H_{AB}^0 for the excited-state and ground-state pathways will be minimized for exchange reactions involving orbitals of similar parentages. This is the case for $Mo_6Cl_{14}^{2-}$/acceptor and donor systems. As Figure 2 illustrates, annihilation involves electrons residing in the metal-based e_g and a_{2g} orbitals of the cluster core. Simple group theoretical treatments reveals that the e_g (HOMO) and a_{2g} (LUMO) molecular orbitals are constructed from the linear combination of d_{xy} orbitals of adjacent metal atoms.[68] These molecular orbitals are shown below. Owing to the similar radial

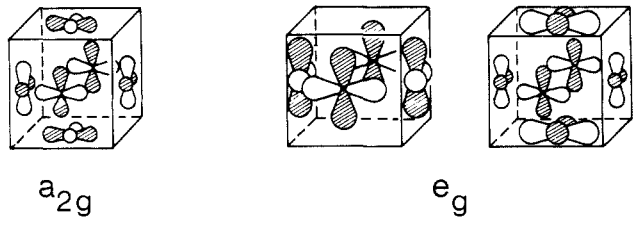

distributions of these metal-based orbitals, the electronic factors of the excited- and ground-state electron-transfer pathways are more closely related than those of any cl or ecl system studied to date. Nevertheless, our assumption of similar values of H_{AB}^0 for the two reaction pathways, at best, is tenuous.

The electron-transfer chemistry of $Mo_6Cl_{14}^-$ and $Mo_6Cl_{14}^{3-}$ ions can be described in terms of two competing reaction channels: a highly exergonic electron-transfer pathway yields ground-state products, and less exergonic exchange leads to the formation of electronically excited $Mo_6Cl_{14}^{2-}$ ion. The ratio of the electron-transfer rates for these two channels, deduced from measurements of ecl yields, is a powerful experimental quantity that has provided us with the opportunity to address fundamental aspects of electron transfer in highly exergonic regions. Specifically, the observation of ecl from $Mo_6Cl_{14}^{2-}$/acceptor and donor systems is evidence of the Marcus inverted region. Moreover, the cl electron-transfer chemistry, interpreted within the context of the theoretical prediction of Marcus and Siders[80] and of Brunschwig, Ehrenson, and Sutin[81] that the electron-transfer rate in the inverted region will accelerate with increasing distance owing to an increase in the solvent reorganizational parameter, suggests that excited-state production yields of less than unity result from facile electron transfer over long distances. These ecl results imply that the most efficient cl or ecl systems will be those possessing annihilation

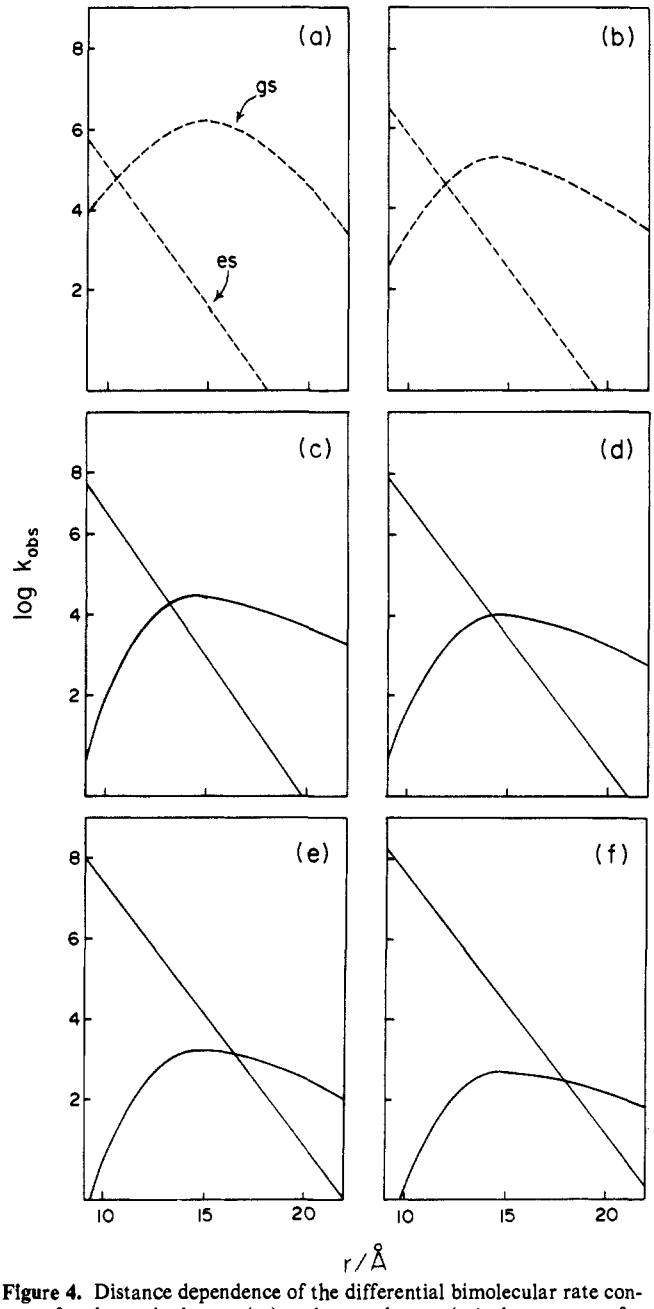

Figure 4. Distance dependence of the differential bimolecular rate constant for the excited-state (es) and ground-state (gs) electron-transfer channels for the reaction of $Mo_6Cl_{14}^-$ with (a) a hypothetical one-electron-reduced pyridinium species with $\Delta G_{gs}^\circ = -2.05$ V and $\Delta G_{es}^\circ = -0.05$ V; (b) a hypothetical one-electron-reduced pyridinium species with $\Delta G_{gs}^\circ = -2.15$ V and $\Delta G_{es}^\circ = -0.15$ V; (c) 4-cyano-*N*-benzylpyridinium; (d) 4-cyano-*N*-methylpyridinium; (e) 4-carbethoxy-*N*-benzylpyridinium; and (f) 4-carbethoxy-*N*-methylpyridinium. The standard free energy driving forces for (c)–(f) are given in Table III.

reactions between redox centers chemically linked over short separation distances.

Acknowledgment. We thank Professor R. I. Cukier for helpful discussions. Financial support from the National Science Foundation (Grant CHE-8705871), the Presidential Young Investigator Program, and a Dreyfus Grant for Newly Appointed Young Faculty in Chemistry is acknowledged. The generous support provided by PYI industrial matching funds from the Dow Chemical Co. is also gratefully acknowledged.

Registry No. Phenothiazine radical cation, 34559-26-7; 10-methoxyphenothiazine radical cation, 34510-35-5; *N,N*-dimethyl-*p*-toluidine radical cation, 77133-47-2; tri-*p*-tolylamine radical cation, 34516-45-5; tris(4-bromophenyl)amine radical cation, 37881-41-7; *p*-benzoquinone radical anion, 3225-29-4; 2,6-dimethyl-*p*-benzoquinone radical anion,

34496-58-7; *p*-dinitrobenzene radical anion, 34505-33-4; *o*-dinitrobenzene radical anion, 34505-38-9; *p*-nitrobenzaldehyde radical anion, 34512-33-9; *m*-nitrobenzaldehyde radical anion, 40951-85-7; 1-chloro-4-nitrobenzene radical anion, 34473-09-1; 5-nitro-*m*-xylene radical anion, 39933-64-7; 3-nitro-*o*-xylene radical anion, 83-41-0; 4-cyano-*N*-benzylpyridinium radical, 113249-25-5; 4-cyano-*N*-methylpyridinium radical, 64365-84-0; 4-carbethoxy-*N*-benzylpyridinium radical, 76036-35-6; 4-carbethoxy-*N*-methylpyridinium radical, 75302-27-1; 4-amido-*N*-benzylpyridinium radical, 113249-26-6; 4-amido-*N*-methylpyridinium radical, 113249-24-4.

Insertion of Two CO Moieties into an Alkene Double Bond To Form a $RCH{=}C(O)C(O){=}CHR^{2-}$ Unit via Organosamarium Activation[1]

William J. Evans* and Donald K. Drummond

Contribution from the Department of Chemistry, University of California, Irvine, Irvine, California 92717. *Received May 11, 1987*

Abstract: RCH=CHR (R = 2-pyridyl) reacts with $(C_5Me_5)_2Sm(THF)_2$ to form a red complex, which reacts with CO at 80 psi in toluene to form $[(C_5Me_5)_2Sm]_2[\mu\text{-}\eta^4\text{-}RCH{=}C(O)C(O){=}CHR]$ (**1**) in 90% yield. **1** cocrystallizes with 2 molecules of toluene in space group $C2/m$ with a = 15.818 (2) Å, b = 14.060 (2) Å, c = 15.353 (2) Å, β = 111.480 (12)°, and Z = 2 for D_{calcd} = 1.32 g cm^{-3}. Least-squares refinement on the basis of 2526 observed reflections led to a final R value of 0.045. The two $(C_5Me_5)_2Sm$ units are bridged by a tetradentate bisenolate ligand, $RCH{=}C(O)C(O){=}CHR^{2-}$, such that each Sm is coordinated to one oxygen and the nitrogen atom of the pyridyl group closest to that oxygen. The Sm–O, Sm–N, and average Sm–C(ring) distances are 2.191 (6), 2.473 (7), and 2.71 (1) Å, respectively.

The divalent organosamarium complex $(C_5Me_5)_2Sm(THF)_2$[2] has proven to have a remarkable reductive chemistry with unsaturated substrates such as C≡O,[3,4] RC≡CR,[4-7] and RN=NR.[8,9] This powerful Sm(II) reagent can induce facile multiple-bond cleavage and reorganization to provide unusual transformations of multiply bonded species. Three examples are shown in eq 1-3. If C=C double bonds could also be transformed in

$$4(C_5Me_5)_2Sm(THF)_2 + 6CO \rightarrow [[(C_5Me_5)_2Sm]_2[\mu\text{-}\eta^3\text{-}O_2CC{=}C{=}O](THF)]_2 + 6THF \quad (1)^3$$

$$2(C_5Me_5)_2Sm(THF)_2 + C_6H_5C{\equiv}CC_6H_5 + 2CO \longrightarrow$$

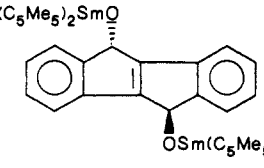

(2)[4]

$$2(C_5Me_5)_2Sm(THF)_2 + C_6H_5N{=}NC_6H_5 + 2CO \longrightarrow$$

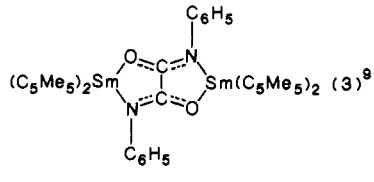

(3)[9]

(1) Reported in part at the 2nd International Conference on the Chemistry and Technology of the Lanthanides and Actinides, Lisbon, Portugal, April 1987, L(II)1.

(2) Evans, W. J.; Grate, J. W.; Choi, H. W.; Bloom, I.; Hunter, W. E.; Atwood, J. L. *J. Am. Chem. Soc.* **1985**, *107*, 941-946.

(3) Evans, W. J.; Grate, J. W.; Hughes, L. A.; Zhang, H.; Atwood, J. L. *J. Am. Chem. Soc.* **1985**, *107*, 3728-3730.

(4) Evans, W. J.; Hughes, L. A.; Drummond, D. K.; Zhang, H.; Atwood, J. L. *J. Am. Chem. Soc.* **1986**, *108*, 1722-1723.

(5) Evans, W. J.; Bloom, I.; Hunter, W. E.; Atwood, J. L. *J. Am. Chem. Soc.* **1983**, *105*, 1401-1403.

(6) Evans, W. J. *Polyhedron* **1987**, *6*, 803-835.

(7) Evans, W. J. In *High Energy Processes in Organometallic Chemistry*; Suslick, K. S., Ed.; ACS Symposium Series 333; American Chemical Society: Washington, DC, 1987; pp 278-289.

(8) Evans, W. J.; Drummond, D. K.; Bott, S. G.; Atwood, J. L. *Organometallics* **1986**, *5*, 2389-2391.

(9) Evans, W. J.; Drummond, D. K. *J. Am. Chem. Soc.* **1986**, *108*, 7440-7441.

Table I. Crystal Data and Summary of Data Collection and Structure Refinement for $(C_5Me_5)_2Sm[\mu\text{-}\eta^4\text{-}(C_5H_4N)CH{=}C(O)C(O){=}CH(C_5H_4N)]Sm(C_5Me_5)_2{\cdot}2C_7H_8$

formula	$Sm_2C_{68}H_{86}N_2O_2$
mol wt	1264.15
space gp	$C2/m$
a, Å	15.818 (2)
b, Å	14.060 (2)
c, Å	15.353 (2)
β, deg	111.480 (12)
V, Å^3	3177
Z	2
D_{calcd}, g/cm^3	1.32
temp, °C	24
λ(Mo Kα), Å	0.71 073; graphite monochromator
μ, cm^{-1}	18.8
min–max transmissn coeff	0.339–0.449
type of scan	θ–2θ
scan width, deg	−1.2 in 2θ from $K\alpha_1$ to +1.2 from $K\alpha_2$
scan speed, deg/min	3
bkgd counting	evaluated from a 96-step peak profile
data collecn range, deg	3–50
total no. of unique data	2955
no. of unique data with $I \geq 3\sigma(I)$	2526
no. of parameters	187
$R(F)$	0.045
$R_w(F)$	0.059
GOF	1.84
max Δ/σ in final cycle	0.39

unusual ways by $(C_5Me_5)_2Sm(THF)_2$, then this organosamarium(II) approach to multiple-bond functionalization would apply to an even wider range of substrates. We report here the samarium-mediated functionalization of a C=C bond in which complete cleavage of the double-bond and double CO insertion is observed.

Experimental Section

The complexes described below are extremely air- and moisture-sensitive. Therefore, both the syntheses and subsequent manipulations of these compounds were conducted under nitrogen with rigorous exclusion of air and water by Schlenk, vacuum-line, and glovebox techniques. The preparation of $(C_5Me_5)_2Sm(THF)_2$ and the methods for drying solvents

0002-7863/88/1510-2772$01.50/0